Electochemical Detection of Imidacloprid Using a Screen Printed Single Walled Carbon Nanotubes Coated with and Ionic Liquids

Karla River-Guzman[1], Lida M. Franco[1], Olimpo García-Beltrán[1], Jorge A. Calderon[2], Edgar Nagles[1]*

[1] Facultad de Ciencias Naturales y Matemáticas, Universidad de Ibagué, Carrera 22 Calle 67, Ibagué 730001, Colombia
[2] Centro de Investigación, Innovación y Desarrollo de Materiales – CIDEMAT, Universidad de Antioquia – UdeA, Calle 70 No. 52-21, Medellín, Colombia
Corresponding Author: Tel.: +57 8 2709400; fax: +5782709443.
[*]E-mail: edgar.nagles@unibague.edu.co

The simple modification of a screen printed single walled carbon nanotubes with ionic liquid 1-butyl-3-metilimidazolium tetrafluorborate allowed the development of a fast and selective methodology to determine imidacloprid (IMI). The morphological and conductive characteristics of the modified surface were analyzed with scanning electron microscopy and electrochemical impedance spectroscopy. The modified surface showed great activity towards the reduction of IMI to -1.2 V. The analytical variables were optimized using linear sweep voltammetry at 0.1 V for 60s, obtaining a limit of detection of 0.21 mg L^{-1}(0.82 µmol L^{-1}). Relative standard deviation with six different electrodes was of 2.6 % (n = 5). Finally, the potential interferers were studied and the sensor was applied in the determination of IMI using samples of commercial honey with recovery between 88.0 and 105.0 % for IMI.

1. INTRODUCTION

Properties present in ionic liquids (ILs) such as; high ionic conductivity, low volatility, large electrochemical window and good electrochemical stability [1], makes them one of the first options in the development of electrochemical sensors. In addition, ILs have been used for the detection of pharmaceutical drugs as promazine [2] and Acetaminophen [3], inorganic substances as sulphites [4], DNA hybridization sensing [5] and metals ions iones such as lead and cadmium [6]. On the other hand, ILs combined with CNTs has been used for the detection of pharmaceutical drugs as carbamazepine

[7], diphenhydramine [8], paracetamol [7], inorganic substances as hidracina [9] and fungicides as pyrimethanil [10]. Zhang et al., have reported the combination of ILs and CNTs are produced by π-π interactions leading to an improvement in the formation of finer networks with other composites, such as oxides of metals, that produces more uniform membranes [5].

Dopamine has been one of the most analyzed substances by electroanalytical techniques using electrodes modified with ILs and CNTs in different types of samples, such as; human serum, human urine and pharmaceutical dosage on a large variety of substrates such as; glassy carbon, carbon paste and screen-printed carbon electrodes [10-17] where the most used cation was imidazolium and the most used anion was hexafluoro phosphate. These works report the benefit of using ILs, such as; large surface area, stability, conductivity, decrease of ΔE for dopamine, making the process faster, extraction effect and good anti-fouling ability.

Imidacloprid named by the IUPAC as (1-(6-chloro-3-pyridylmethyl)-N-nitroimidazolidin-2-ylideneamine) was classified as a neonicotinoid pesticides. Widely used in agricultural production due to its great insecticidal activity [18]. It mainly affects the central nervous system of insects [19]. On the other hand, superficial properties of the soil can prevent the adsorption of the residues of IMI [20], contaminated the groundwater causing problems to people's health. Hence, the development of a selective and sensitive methodologies for the determination of IMI is important. Electrotroanalytic techniques have been used in the last two decades to detect IMI with a variety of modified electrodes (Table 1). These works have proven to be sensitive, selective and easy to produce. Some ILs such as; 1-Allyl-3-methylimidazolium tetraflouroborate on carbon-ceramic electrode have been used for the detection of IMI by electroanalytical techniques with a detection limit of 0.031 μmol L^{-1}. Authors attributed to the large capacitive current resulting from the ionic nature of the ionic liquid and the increasing surface area of the modified electrode [21], by UV-Vis spectroscopy was used 1-propylamino-3-methylimidazolium tetrafluoroborate with a detection limit of 0.08 μMol L^{-1}, but the authors do not explain the effect of ILs on the reduction of IMI [22]. There are few reports to detect IMI using ILs with CNTs. Recently, Zhao et al., Have reported the combined use of ILs with CNTs on molecularly imprinted polymers for IMI with a detection limit of 0.08 μMol L^{-1}, but the authors do not explain the effect of ILs on the reduction of IMI [23].

The aim of this work is the development of a sensor for detection of IMI using ILs, supported on a single walled-screen printed carbon nanotubes electrode (SWCNT/SPC) and it evaluates their performance in the detection of IMI in honey samples. Results allowed the detection of IMI with SWCNT/SPC and IL allowed a detection limit (less than 1.0 mg L^{-1}) using simple electroanalytical techniques, as linear sweep voltammetry. Therefore, it allows the use of cheaper devices since it is not necessary to use pulse voltammetry.

2. EXPERIMENTAL PART

2.1 Reagents and instruments.

Water was obtained from Purifier System Wasselab ASTM D1193. Imidacloprid standard solutions 78.22 μmol L^{-1} and 5.0 μmol L^{-1} were prepared once only, for the entire study from pure reagent (Sigma-Aldrich). The buffer solutions were prepared from H_3PO_4, NaH_2PO_4 and $NaHPO_4$

(Merck), adjusting the pH required with NaOH and HNO_3 0.5 mol L^{-1}. KCl, K_4FeCN_6 and 1-butyl-3-methylimidazolium tetraflouroborate were obtained from Sigma-Aldrich. Cyclic and linear sweep voltammograms were obtained using a potentiostat DropSens μStat 400. A Versa STAT 3 Potentiostat/galvanostat from Princeton-Applied Research was used to develop the Electrochemical Impedance Spectroscopy (EIS) measurements. The surface of the electrodes was characterized by Scanning Electron Microscopy (SEM) using JEOL JSM 6490 LV equipment. The electrochemical cell was constituted by a system of three incorporated screen-printed electrode (DRP C110, DRP-110 SWCNT DropSens, Oviedo, Spain) with a working electrode of carbon (4 mm), Ag pseudo reference electrode and carbon as counter electrode.

2.2 Measurement procedure.

2.2.1 Scanning Electron Microscopy

The surface of the electrodes was characterized by Scanning Electron Microscopy (SEM) using a JEOL JSM 6490 LV equipment.

2.2.2 Voltammetry and electrochemical impedance spectroscopy analysis.

Cyclic voltammetry analysis was developed with $K_4Fe(CN)_6$ 10.0 mmol L^{-1} in KCl 10.0 mmol L^{-1}. Cyclic voltammograms were recorded, while the potential was scanned from -0.3 to 1.0 V with scan rate of 100.0 mV s^{-1}. For IMI, in the electrochemical cell was added 9.5 mL of type A water with 0.5 mL PBS and 0.250 mL IMI (50.0 μmol L^{-1}). Cyclic voltammograms were recorded, while the potential was scanned from -0.80 to -1.6 V with scan rate of 50.0 mV s^{-1}. Each cyclic voltammograms were repeated for three times. Linear sweep voltammograms were developed by direct addition of 20 μL of PBS and 10 μL of IMI (5.0 μmol L^{-1}) on the modified electrode surface. It was possible to add almost ten IMI additions on modified electrode. Subsequently, IMI was scanned between 1.0 and 80.0 μmol L^{-1} at 0.1 V by 60 s.

Electrochemical Impedance Spectroscopy (EIS) measurements were performed to study the electrochemical response of the modified electrodes with $K_4Fe(CN)_6$ as electrolyte. EIS measurements were carried out at the open circuit potential using perturbation amplitude of 10 mV and a frequency range between 10.0 kHz and 0.10 Hz. The working electrodes were: screen-printed carbon (SPC), SPC with single-walled carbon nanotubes (SWCNT/SPC) and SWCNTSPC with $BMIMBF_4$ (IL-SWCNT/SPC) electrodes.

2.2.3 Treatment of samples

The honey for experiment was obtained from five hives exposed during four months to honey syrup (sugar + water and honey) with a residual formulation of imidacloprid, the bees were fed twice a week. The honey produced by the bees exposed to insecticides was collected in plastic recipients and stored to – 4°C for further analysis. 300 ml of the honey were treated with a mixture of water and 100

ml of acetonitrile to extract the organic fraction. This fraction was concentrated under reduced pressure in a vacuubrand system.

2.3 Modified electrode Preparation (chitosan-SWCNT-IL/SPCE)

Before each modification, the SPC and SWCNT/SPC were washed with buffer solution pH 7.0 and was dried using hot air stream. 10µL of IL (pure) was deposited by drop casting on the electrodes surfaces. Immediately, it was left at $60^{o}C$ for one hour, and then washed to remove excess solvent. The newly prepared electrode was treated with 10 cycles with CV between 0.0 and 1.0 V at 100.0 mV s^{-1} to obtain a more homogeneous surface.

3. RESULTS AND DISCUSSION

3.1 SEM analysis of the SPC, SWCNT/SPC and IL-SWCNT/SPC electrodes
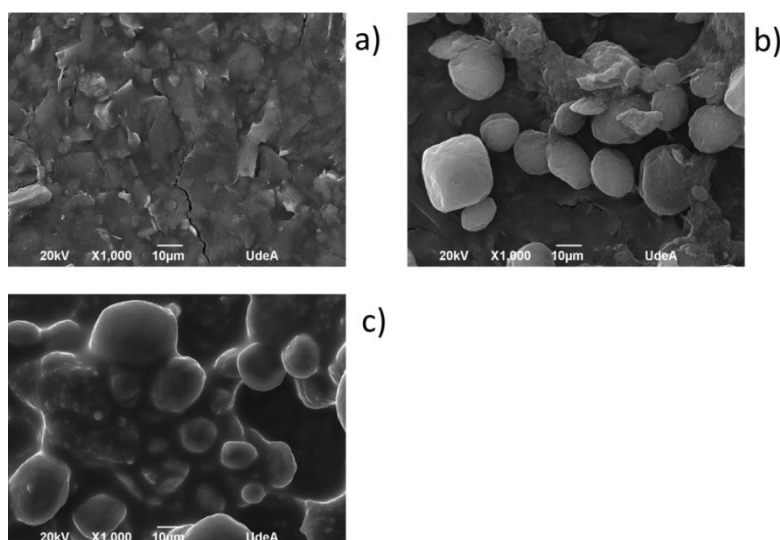

Figure 1. SEM images of a) SPC, b) SWCNT/SPC and c) IL-SWCNT/SPC electrodes.

Characterization of the surface for each electrode SPC, SWCNT/SPC and IL-SWCNT/SPC electrodes were developed to demonstrate the presence of IL (BMIMBF$_4$) on the surface of the modified electrode. Results are presented in figure 1. The typical smooth and cracked layer in the form of leaves is observed for the SPC electrode (fig 1a). While, for the SWCN /SPC electrode (Fig. 1b), a series of globules is observed which is the common form of the nanotubes. A less aggravated surface is observed. On the surface treated with IL (Fig. 1c), it is clearly observed that the nanotube globules have been completely covered by IL. Furthermore, the cracks have been eliminated. Similar results were reported using SEM images with five times more increase in dopamine detection using chitosan-IL-SWCNT/SPC electrode [17].

3.2. Voltammetry analysis of the SPC, SWCNT/SPC, and IL-SWCNT/SPC electrodes using K₄Fe(CN)₆
by cyclic voltammetry.

Electrochemistry property of SPC, SWCNT/SPC and IL-SWCNT/SPC were studied using $K_4Fe(CN)_6$ and KCl 10.0 mmol as electrolyte test. The voltammograms are shown in fig. 2A. The value of ΔE for SPC was 400.0 mV. Anodic and cathodic peak currents were 97.76 and -68.06 µA, respectively. The value of ΔE decreased to 320.0 V with SWCNT/SPC and the anodic and cathodic peak currents were increased to 143.8 and -188.86 µA, respectively. The increase in currents was almost 67% and the difference of anodic and cathodic peak currents was 13 µA. In addition, when SWCNT-SPC was modified with IL, the ΔE decreased to 208.0 V with anodic and cathodic peak currents of 197.92 and -188.33 µA. Anodic and cathodic peak currents showed an increase of almost 90.0% compared to the unmodified SPC electrode. On the other hand, the difference of anodic and cathodic peak currents was 9.0 µA. These results indicate that the presence of IL on the surface of SWCNT/SPC electrode improves charge transfer, making a quasi-reversible system that requires less energy compared to electrodes without IL. Using other electrodes, such as glassy carbon and carbon paste modified with carbon nanotubes and IL, a ΔE less than 100 mV was reported. It indicated that the surface of glassy carbon and carbon paste are more active [12, 13]
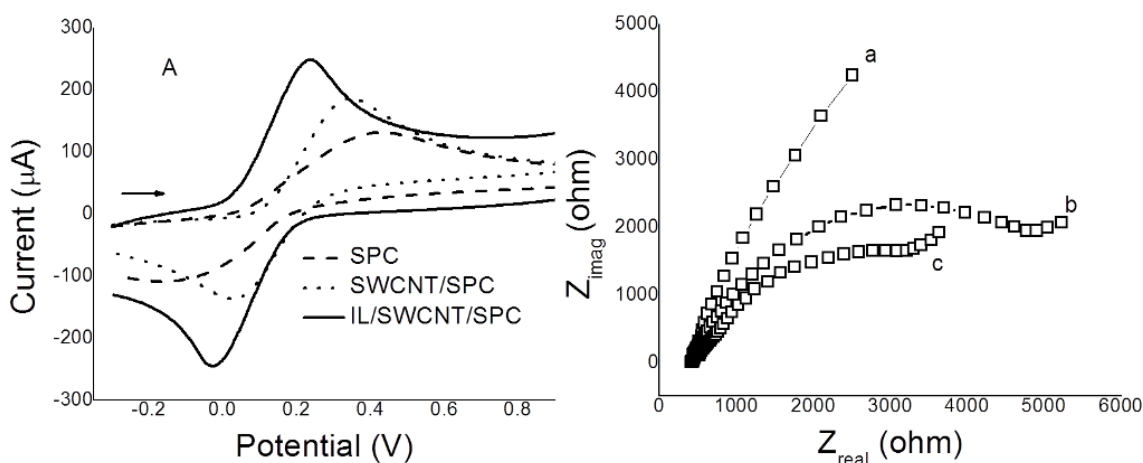

Figure 2. A) Cyclic voltammograms on SPC (---), SWCNT/SPC (···) and IL-SWCNT/SPC (—) electrodes. B) Nyquist diagrams on SPC (a), SWCNT/SPC (b) and IL-SWCNT/SPC (c) of $K_4Fe(CN)_6$ 10.0 mmol L^{-1} in KCl 10.0 mmol L^{-1}.

3.3 Electrochemical Impedance analysis of the SPC, SWCNT/SPC and IL-SWCNT/SPC electrodes
using K₄Fe(CN)₆.

EIS is a useful technique to investigate the properties on the surface of modified electrodes. Results are normally reported in a plot called Nyquist, where real resistance (Z´) is plotted vs imaginary resistance (Z´´) for an electrical circuit to high and low frequencies. The charge transfer limitation process, and the charge transfer resistance (Rct) values can be measured directly as the diameter of the semicircle observed at high frequencies in Nyquist diagrams [24]. Fig. 2B shows the

Nyquist diagrams of the electrochemical impedance measurements performed in 10.0 mmol L^{-1} $K_4Fe(CN)_6$ in 10.0 mol L^{-1} KCl using SPC (a), SWCNT/SPC (b), and IL-SWCNT/SPC (c) electrodes. SPC electrode exhibits Rct value of 8000 Ohm. Similar situation has been reported for bare GC electrode in $Fe(CN)_6^{3-/4-}$ containing 10.0 mmol L^{-1} KCl [25]. Nyquist diagrams of the electrodes SWCNT/SPC and IL-SWCNT/SPC the Rct values decreased considerably. Moreover, they presented a semicircle of smaller diameter with a slope close to 45° at low frequencies, which is associated with the semi-infinite diffusion type Warburg impedance. These results demonstrate the effectiveness of SWCNT and IL combination to improve the conductive properties of SPC electrode. On the other hand, these results were similar to those observed with CV (section 3.3).

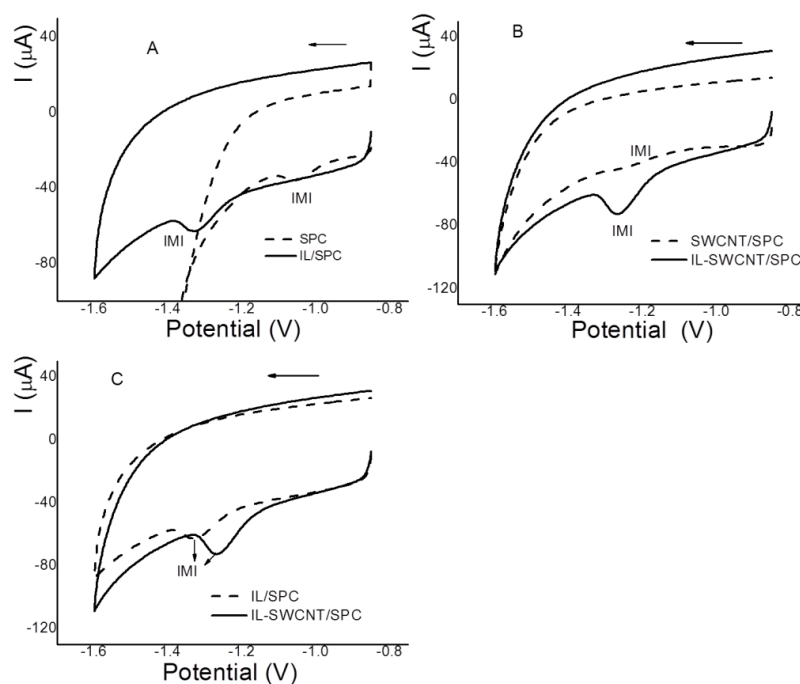*3.4 electrochemical reduction of IMI on SPC, SWCNT/SPC and IL-SWCNT/SPC electrodes.*

Figure 3. Cyclic voltammograms for IMI 19.0 µmol L^{-1} on (A) SPC (---), IL/SPC (—), (B) SWCNT/SPC (···), IL-SWCNT/SPC (—) and (C) IL/SPC (···), IL-SWCNT/SPC (—) electrodes. PBS 0.01 mmol L^{-1}. Scan rate 50.0 mV s^{-1}.

The electrochemical reduction reaction of IMI occurs through the reduction of the nitro-NO_2 group of the chemical structure of IMI by producing hydroxylamine derivatives [24-26]. With the objective to select the optimal electrode support that shows the highest activity on this reaction for IMI, the reduction of IMI 19.0 µmol L^{-1} on SPC, IL/SPC, SWCNT/SPC and IL-SWCNT/SPC electrodes was studied. The voltammograms are shown in Fig. 4. Using SPC electrode, (curve 2A ---), potential cathodic peak for IMI was observed at -1.05 V with cathodic peak current of -5.10 µA. This potential value was similar to those reported using BiF [26], graphene oxide [24] and nafion/TiO_2 [27]. Using SWCNT/SPC electrode (curve 2B ---) no signal was observed for the reduction reaction. On the other hand, when SPC and SWCNT/SPC electrodes were treated with IL (curves 2A-B—) the

reduction signal for IMI increased to -10.97 and -18.63 μA, respectively. In addition, the signal changed to more positive potential values of 1.3 and 1.26 V, respectively. Figure 2C shows that SWCNT/SPC electrode treated with IL showed greater activity towards IMI reduction reaction, where cathodic peak current increased almost 27.0% and the potential was observed at less positive values. Possibly, the interaction between IL and IMI is more stable, compared with other substrates such as; polymers [23]. Therefore, it requires more energy for IMI reduction. It was evident that the presence of IL in the carbon nanotube network improved the activity of the surface and allowed the reduction of IMI more effective, compared to the SPC without CNTs. IL-SWCNT/SPC electrode was selected for further studies.

3.5 pH study for IMI using IL-SWCNT/SPC electrode.

pH for reduction reaction of IMI was studied to find the highest cathodic peak currents with 19.0 μmol L^{-1} using IL-SWCNT/SPC electrode with PBS electrolyte between 3.0 and 8.0 pH values. Voltammograms for cathodic peak currents between pH 3.0 and 7.0 values and linear relationship between pH and peak current are shown in the fig. 7. Clearly, it was seen that cathodic peak currents increased from 5.0 at 7.0 pH values. At higher pH values, cathodic peak current decreased considerably. With other modified electrodes, such as Copper (II) phthalocyanine on carbon ceramic electrode [24], graphene oxide on glassy carbon electrode [24], and poly (carbazole)-reduced graphene on glassy-carbon electrode [27] was chosen a pH value close to 7.0 as optimal. For this reason, a pH 7.0 solution is chosen for further studies.
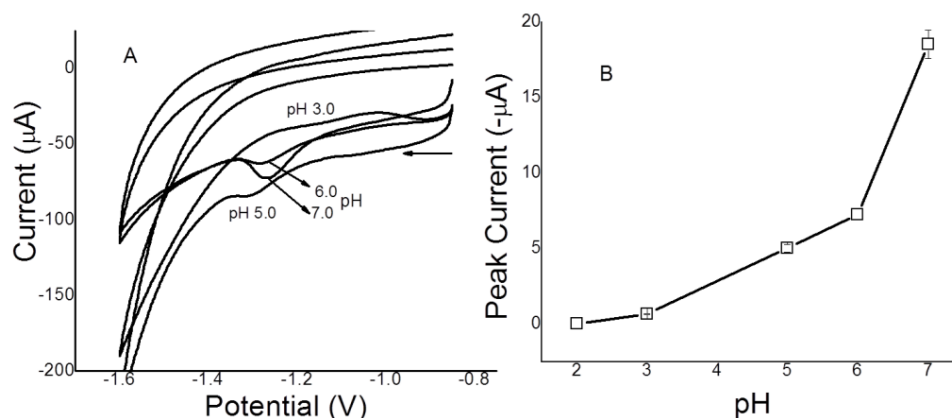

Figure 4. (A) Voltammograms of the Effect of pH on chatodic peak currents for IMI 19.0 μmol L^{-1} using IL-SWCNT/SPC (B) plot of reduction peak current vs pH. PBS 0.01 mmol L^{-1}. Scan rate 0.05 mV s^{-1}.

3.6 Effect of scan rate for IMI using IL-SWCNT/SPC electrode.

Scan rate was investigated by cyclic voltammetry with scan rate between 70.0-160.0 mV s^{-1} to determine which process is involved in the transport of mass in the reduction- reaction of IMI 19.0

μmol L^{-1} using IL-SWCNT/SPC. Fig 5 showed that cathodic peak currents increased proportionally as the increase of the scan rate from 70 to 160 mV s^{-1}. Regression equation for cathodic peak currents was I_{pc}= -1.308 + 0.08535v (correlation coefficient R^2=0.990). This result indicates that the process is controlled by adsorption. Possibly, ILs acts as an extractor agent. Similar results were reported for IMI using reduced graphene on glassy carbon electrode without ILs [27]. Moreover, using ILs with carbon-ceramic electrode, a process controlled by diffusion for IMI was reported [3]. Therefore, the properties of the ILs will depend, to a large extent, on the substrate where the ILs is deposited.
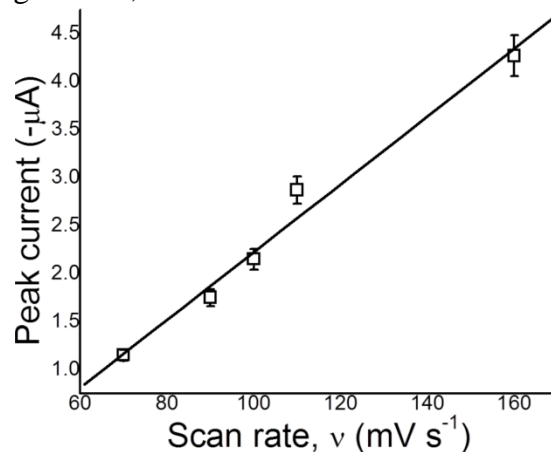

Figure 5. Plot for peak current (-μA) vs scan rate ν (70.0-160 mVs^{-1}) for IMI 19.0 μmol L^{-1} using IL-SWCNT/SPC. Conditions: pH: 7.0. PBS (0.01mmol L^{-1})

3.7 Study in function of adsorption time for ILs, reproducibility and stability for SWCNT/SPC electrode.
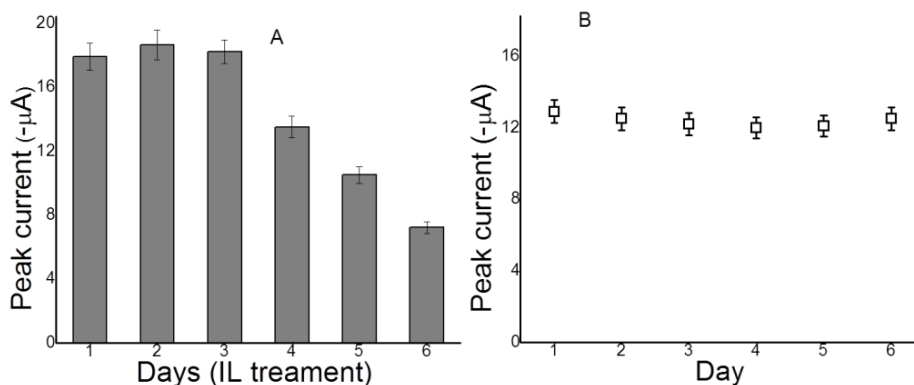

Figure 6. (A) Plot of peak current versus number of days for IL treatment (B) Plot of peak current versus number of days of six different electrodes for IMI 19. μmol L^{-1} in 7.0 pH PBS using IL-SWCNT/SPC. Linear sweep voltammetry at 0.10 V by 60.0 s.

Performed studies showed that cathodic peak current for IMI changed as a function of the time of deposition of ILs on SWCNT/SPC electrode. Figure 6A shows the cathodic peak currents for IMI as a function of the ILs deposit time. Results showed that the current was more stable after three days of ILs deposition at 60°C. At higher days, cathodic peak current decreases exponentially. Possibly, the

surface of SWCNT/SPC is saturated and forms a surface that blocks the transfer of charge. Two-days deposit of ILs at 60°C was chosen as optimal. **Fig. 6B** shows the plot of cathodic peak currents versus the number of days for 19.0 µmol L^{-1} of IMI in 7.0 pH PBS solution using six IL-SWCNT/SPC electrodes. Results showed a good reproducibility of 2.6% calculated as the relative standard deviation. The stability of the modified electrode was studied with the same modified electrode used for IMI reduction for six days. Results showed that the same electrode cannot be used for more than two measurements without suffering a considerable loss of activity.

3.8 Detection limit for IMI using IL-SWCNT/SPC electrode.

Detection limit was calculated for IMI from calibration curves prepared with several additions of 10 µL of IMI on IL-SWCNT/SPC surface electrode with 20.0 µL of BPS pH 7. Fig. 7A-B shows the linear sweep voltammograms and calibration curve for IMI. Experimental conditions: pH 7.0 at 0.10 V by 60.0 s. Equation curve Ip = -9.422 + 2.11C_{IMI} (correlation R^2= 0.989) with Detection limits (3σ/b) where σ is the random error in x and y, and b is the slope [28] was 0.21mg L^{-1} (0.84 µmol L^{-1}) for IMI. In table 1, different methodologies for IMI with detection limits between 0.020 and 2.93 µmol L^{-1} using electrodes modified with greater rigor were reported. These results indicate that IL-SWCNT/SPC electrode present an acceptable detection limit.
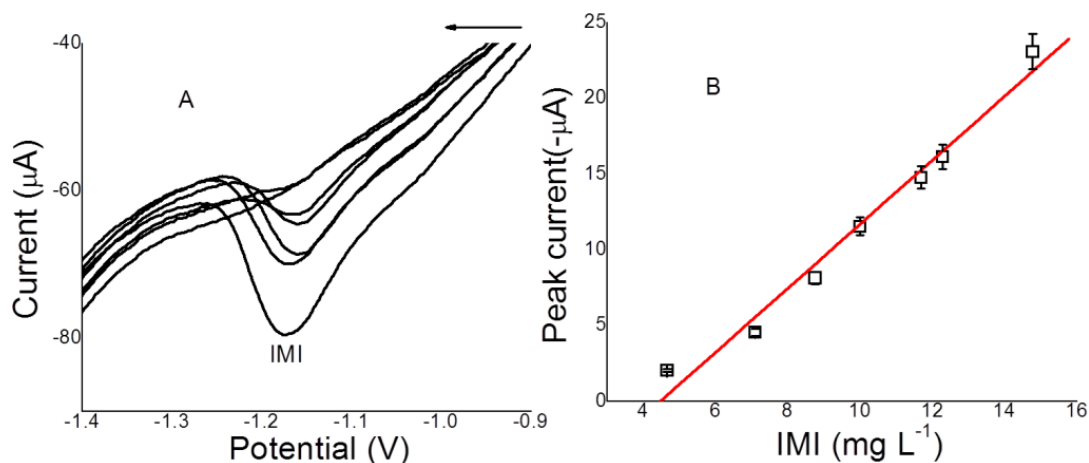

Figure 7. (A) Linear sweep voltammograms and (B) calibration curve for IMI 2.80 to 14.70. mg L^{-1} using IL-SWCNT/SPC electrode. Conditions: pH: 7.0 at 0.10 V by 60.0 s. Scan rate 100.0 mV s^{-1}.

3.9 Interference study

The possible effect of some metal ions on the reduction reaction of IMI was analyzed using ICP multi-element standard solution IX (Merck) containing As, Be, Cd, Cr (VI), Hg, Ni, Pb, Se and Tl 100 mg L^{-1}. The effect of some organic substances such as thimerosal (TIM), endosulfan (END), rutin (RT), morin (MO), tartrazine (TZ) and amaranth (AM) was also evaluated. Results are shown in Figure 8. It was clearly observed that these substances do not cause any kind of interference with reduction reaction for IMI.
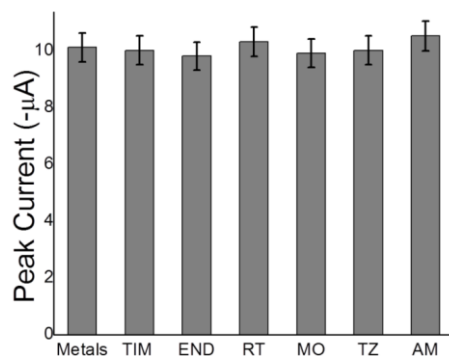
Figure 8. (A) Plot of peak current versus number of IMI 19.0 μmol L^{-1} in presence of metals ions, TIM, END, RT, MO, TZ, AM 0.34 mmol L^{-1} using IL-SWCNT/SPC. Conditions as fig 6.

Table 1. Some modified electrodes used in the detection of IMI.

Electrode	Materials	DL´s μmol L^{-1}	Application	Ref.
GCE CPE	BiF	2.93		[29]
GCE	β-CDP/rGO	0.02		[24]
CCE	CuPc	0.28	Commercial formulation, Tomato samples	[26]
GCE	AgnN/TiO$_2$nN	0.93	Commercial formulation	[30]
GCE	PCz/CRGO	0.22		[27]
CCE	AMIM-BF$_4$	0.031	Agricultural products Rice samples	[3]
CPE	MIP	0.10		[31]
GCE	MIP	0.40	Fruit samples	[32]
GCE	MIP	0.08	Fruit samples	[23]
CPE	Tricresyl phosphate,	0.52	Commercial formulation	[33]
SWCNT-SPC	IL	0.84	Honey	[This work]

DL´s: detection limits; GCE: glassy carbon electrode; CCE: carbon-ceramic electrode; CPE: carbon paste electrode; BIF: Bismuth film; SWCNT-SPC: Screen printed single walled carbon nanotube electrode; β-CDP/rGO: Reduced-graphene oxide modified with β-cyclodextrin polymer; CuPc: copper(II) phthalocyanine; AgnN/TiO$_2$nN: nanosilver-Nafion/nanoTiO$_2$-Nafion; PCz/CRGO: Polycarbazole reduced graphene oxide; MIP: molecularly-imprinted polymers¸ AMIM-BF$_4$: 1-Allyl-3-methylimidazolium .

3.9 Validation study

The sensor accuracy was checked in the determination of IMI in commercial honey samples spiked with known amounts of IMI. Results are summarized in table 1 and the voltammograms and

calibration curve of sample 1 are shown in figure 9. Results showed a relative error of less than 10.0%. These results indicate that the sensor has appropriate accuracy at high and low concentrations of IMI. On the other hand, the reduction potential for IMI was observed at more positive potential values, possibly due to an effect of the matrix in the sample.

Table 2. Results for commercial honey samples spiked with known amounts of IMI.

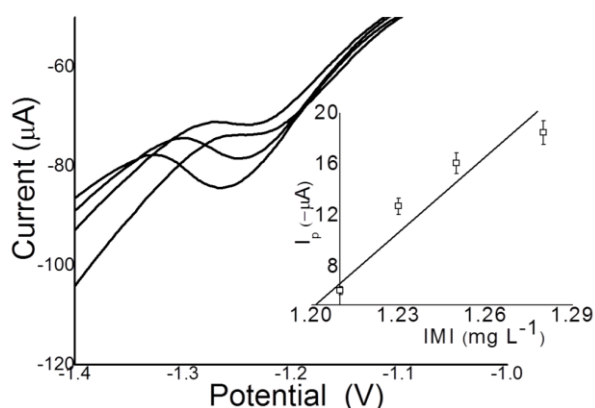| Sample	Added (mg L^{-1})	Found (mg L^{-1})	% Relative error
*1	1.21	1.15	-4.95
2	60.0	65.78	9.63

*Voltamperograms and calibration curve in figure 9

Figure 9. Linear sweep voltammograms and calibration curve (insert) for sample 1, table 2. Using IL-SWCNT/SPC electrode. Conditions as fig 6.
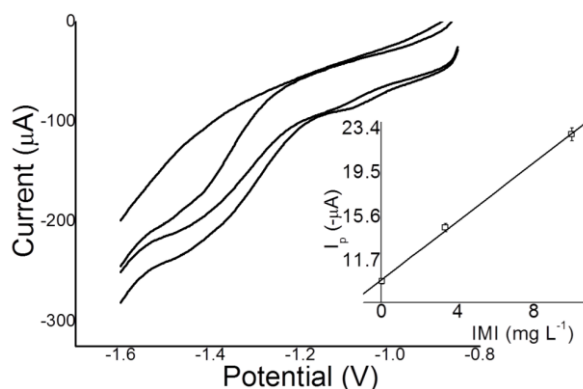
3.10 Analytical applications

Figure 10. Linear sweep voltammograms and calibration curve (insert) for IMI in honey sample 1 (table 3) using IL-SWCNT/SPC electrode. Conditions as fig. 9.

The utility of the sensor was proven in the detection of IMI in samples of honey produced by bees without IMI and treated with known quantities of IMI. Results are summarized in Table 3. The results indicate that the amount of IMI adsorbed by the bees transfers to the honey produced [34]. On

the other hand, the values are below of the no-observed-adverse-effect level (NOAEL) by Food and Agriculture Organization of the United Nations (FAO) [35]. In addition, honey samples 3 and 4 without IMI treatment was not detected. The samples were analyzed by HPLC detecting IMI < 10.0 mg L^{-1}

Table 3. Results for honey samples with IMI treatment and without IMI treatment.

Sample	Added (mg L^{-1})	Found (mg L^{-1})	Recovery (%)
*Honey treated with IMI	-	4.71±0.3	-
Honey treated with IMI	-	3.53±0.1	-
Honey treated with IMI	-	4.82±0.9	-
Honey without IMI	3.30	2.90±0.8	88.0
Honey without IMI	3.30	3.5±0.5	105.0

*Voltammograms and calibration curve showed in the figure 10

4. CONCLUSIONS

The reduction reaction of IMI on a single walled screen-printed carbon nanotubes electrode coated with IL allowed the development of a simple methodology to detect IMI in honey samples. The presence of IL increased the cathodic peak current almost a 27.0% compared with SPC electrode without IL. This new methodology proved to be almost sensitive compared with commonly used methodologies. It showed to be cheaper and easy to produce.

References

1. D. Wei, A. Ivaska, *Anal. Chim. Acta*, 607 (2008) 126.
2. V. Arabali, M. Ebrahimi, H. Karimi-Maleh, *Chinese Chem. Lett.*, 27 (2016) 779.
3. M. R. Majidi, M. H. Pournaghi-Azar, R. F. B. Baj, *J. Mol. Liq.,* 220 (2016) 778.
4. H. Beitollahi, S. Tajik, P.Biparva, *Measurement*, 56 (2014) 170.
5. W. Zhang, T. Yang, X. Zhuang, Z. Guo, K. Jiao, *Biosens. Bioelectron.,* 24 (2009) 2417.
6. E. Nagles, V. Arancibia, R. Ríos, C. Rojas, *Int. J. Electrochem. Sci.*, 7 (2012) 5521.
7. L. Daneshvar, G, Rounaghi, Z. E'shaghi, M. Chamsaz, S. Tarahomi, *J. Mol. Liq.,* 215 (2016) 316
8. S. Cheraghi, M. A. Taher. *J. Mol. Liq.,* 219 (2016) 1023.
9. M. Mazloum-Ardakani, A. Khoshroo, *Electrochim. Acta*, 103 (2013) 77.
10. J. Yang, Q. Wang, M. Zhang, S. Zhang, Lei Zhang, *Food Chem.*, 187 (2015) 1.
11. M. Noroozifar, M. Khorasani-Motlagh, M. B. Parizi, R. Akbari, *Ionics* 19 (2013) 1317.
12. Y. Zhao, Y. Gao, D. Zhan, H. Liu, Q. Zhao, Y. Kou, Y. Shao, M. Li, Q. Zhuang, Z. Zhu, *Talanta* 66 (2005) 51.
13. A. Afraz, A. A. Rafati, M. Najafi, *Mat. Sci. Eng. C* 44 (2014) 58.
14. Y. Sun, J. Fei, J. Hou, Q. Zhang, Y. Liu, B. Hu, *Microchim. Acta*, 165 (2009) 373.
15. A. A. Rafati, A. Afraz, A. Hajian, P. Assari, *Microchim. Acta,* 181 (2014) 1999.
16. X. Niu, W. Yang, H. Guo, J. Ren, J. Gao, *Biosens. Bioelectron.*, 41, (2013) 225.

17. E. Nagles, O. García-Beltrán, J. A. Calderón. *Electrochim. Acta,* 258 (2017) 512.
18. B. Dalibor, M. Cedomila, *J. Environmen. Sci. Health: Part B*, 47 (2012) 779.
19. V. Guzsvány, Z. Papp, J. Zbiljić, O. Vajdle, M. Rodić, *Molecules*, 16 (2011) 4451.
20. S. K. Papiernik, W. C. Koskinen, L. Cox, P. J. Rice, S. A. Clay, N. R. Werdin-Pfisterer, K. A. Norberg.. *J. Agric. Food Chem.*, 54 (2006) 8163.
21. R.Majidi, R. Baj, M. Bamorowat, *Measurement,* 93 (2016) 29.
22. X. Zhang, Z. Sun, Z. Cui, H. Li, *Sensor. Actuat. B Chem.*, 191 (2014) 313.
23. L. Zhao, J. Yang, H. Ye, F. Zhao, B. Zeng.. *RSC Adv.*, 7 (2017) 4704.
24. V. Guzsvany, M. Kadar, Z. Papp, L. Bjelica, F. Gaal, K. Toth, *Electroanalysis,* 20 (2008) 291.
25. E. Nagles, J. A. Calderón, O. García-Beltrán, *Electroanalysis,* 29 (2017), 1081.
26. R. Majidi, K. Asadpour-Zeynali, M. Bamorowat, M. Nazarpur. *J. Chinese Chem. Soc.*, 58 (2011), 207.
27. W. Lei, Q. Wu, W. Si, Z. Gu, Y. Zhang, J. Deng, Q.Hao, *Sensor. Actuat. B Chem.,* 183 (2013) 102.
28. J. Mocak, A.M. Bond, S. Mitchella, G. Scollary. *Pure Appl. Chem.,* 69 (1997) 297.
29. M. Chen, Y. Meng, W. Zhang, J. Zhou, J. Xie, G. Diao, *Electrochim. Acta,* 108 (2013) 1.
30. A. Kumaravel, M. Chandrasekaran, *Sensor. Actuat. B Chem.*, 158 (2011) 319.
31. M. Zhang, H. T. Zhao, T. J. Xie, X. Yang, A. J. Dong, H. Zhang, J. Wang, Z. Y. Wang, *Sensor. Actuat. B Chem.*, 252 (2017) 991.
32. L. Kong, X. Jiang, Y. Zeng, T. Zhoua, G. Shi, *Sensor. Actuat. B Chem.*, 185 (2013) 424.
33. Z. Papp, I. Švancara, V. Guzsvány, K. Vytřas, F. Gaál, *Microchimica Acta*, 166 (2009) 169.
34. E. A. DMitchell, B. Mulhauser, M. Mulot, A. Mutabazi, G. Glauser, A. Aebi, *Science*, 358 (2017) 109.
35. Food and Agriculture Organization of the United Nations. Pesticide residues in food 2006 Joint FAO/WHO Meeting on Pesticide Residues. Report of the Joint Meeting of the FAO Panel of Experts on Pesticide Residues in Food and the Environment and the WHO Core Assessment Group on Pesticide Residues Rome, Italy, 3–12 October 2006